Evolutionary Ecology Research, 2002, **4**: 811–841

Effects of Oligo-Miocene global climate changes on mammalian species richness in the northwestern quarter of the USA

Anthony D. Barnosky* and Marc A. Carrasco

Department of Integrative Biology and Museum of Paleontology, University of California, Berkeley, CA 94720, USA

ABSTRACT

We derived species richness curves using three different methods for mammal species recorded in fossil deposits between 30 million and 9 million years old (late Oligocene through late Miocene) for three geographic regions in the USA: the Northwest, northern Rocky Mountains and northern Great Plains. The data were used to examine the relationship between global climate change and species richness at the regional scale. Our goal was to test the hypothesis that geographic scaling issues account for the lack of correlation that has been observed between continental species richness and the oxygen–isotope curve. The results of all three methods used in this study suggest that species richness in the three regions analysed did not change in response to the global temperature signal, supporting the inferences drawn from continental-scale analyses. The most prominent signal is a peak in species richness in the Rocky Mountain region about 15 million years ago, possibly due to increased beta diversity within the mountains, although many of these species were shared between all three biogeographic provinces. This peak coincides with the Mid-Miocene Climatic Optimum, but it appears unlikely that global temperature change was the direct cause because no response in species richness characterized the even greater Late Oligocene Warming. The Mid-Miocene richness peak also closely follows the onset of major tectonic events in the Rocky Mountain region, which may have led to increased within-province endemism through a combination of physiographic and related climatic effects not recorded in the global temperature signal, a hypothesis that deserves detailed testing.

Keywords: climate change, mammals, Miocene, Oligocene, palaeontology, species richness.

INTRODUCTION

Many workers have discussed the effect of climate change on species richness patterns through geological time (see, for example, citations in Rosenzweig, 1995). For mammals, assessing this effect has remained elusive, with some workers claiming global changes in climate have little influence on species richness (most recently, Alroy *et al.*, 2000) and others

* Author to whom all correspondence should be addressed. e-mail: barnosky@socrates.berkeley.edu

inferring that climate changes profoundly affect species richness patterns (for example, Janis *et al.*, 2000; Barnosky, 2001). Recent work has suggested that scaling issues are at the heart of different interpretations about how global climate change affects mammalian species richness (Barnosky, 2001). Briefly stated, the scaling argument posits that studies lumping data from several different climatic zones spread over large continents will always show no response to global climate change. This is because global changes manifest in different directions from region to region, as documented by general circulation models and modern weather observations (National Assessment Synthesis Team, 2001). On the other hand, data compiled from single climatic zones have the potential of revealing a biotic response to global climate changes, because all of the species within the single climate zone experience the same effect of the global climate change, whether or not it is in the same direction as the global mean.

Here we test whether geographic scaling issues explain an apparent absence of correlation between species diversity of mammals in the conterminous United States and global temperature change inferred from the oxygen–isotope curve (Alroy *et al.*, 2000). In general, the data reported here support the lack of correlation. For the data set analysed, the biggest increases in mammalian species richness came not with the biggest warming event recorded in the oxygen–isotope curve, but with the onset of a tectonic event that geographically fragmented the landscape. However, complicating the interpretation is the fact that different assumptions about the data lead to markedly different interpretations about species richness, highlighting the need for critical evaluation of both field relationships and statistical techniques in deriving species richness estimates from palaeontological data sets.

METHODS

The temporal focus of this study was on the late Oligocene through the late Miocene (30 to 9 million years ago) encompassing the Arikareean through the Clarendonian North American Land Mammal Ages. The oxygen–isotope curve compiled by Zachos *et al.* (2001) provided a proxy of global climate change (Fig. 1). We deemed this proxy to be the most suitable for our purpose of assessing the globally averaged temperature signal because the curve of Zachos *et al.* used information from at least 42 DSDP and ODP cores distributed through the Atlantic (18 cores), Pacific (14 cores) and Indian (10 cores) Oceans. The oxygen–isotope curve records a signal of global temperature change and global ice volume. For the purposes of this paper, the relative temperature scales of Zachos *et al.* (2001) and Miller *et al.* (1987) were accepted, both of which suggest a 4°C change in global temperature for every 1‰ change in $\delta^{18}O$, although interpretations of absolute temperature vary with ice volume. The isotope record shows two global warming events: one spanning 27 to 24 million years (Late Oligocene Warming) and one of slightly longer duration but of lower magnitude from about 18 to 14 million years (Mid-Miocene Climatic Optimum, also known as the late-Early Miocene Climatic Optimum in earlier papers). These warming events indicated by the curve of Zachos *et al.* also appear in other syntheses of oxygen–isotope data (see, for example, Miller *et al.*, 1987) as well as in individual cores with high stratigraphic resolution from different parts of the world (see, for example, Miller and Fairbanks, 1985; Mutti, 2000).

Changes in Oligo-Miocene species richness were calculated for three different geographic regions in the northwestern United States: the Northwest, the northern Rocky Mountains and the northern Great Plains (NW, MT and PL in Fig. 2). Today, these regions roughly

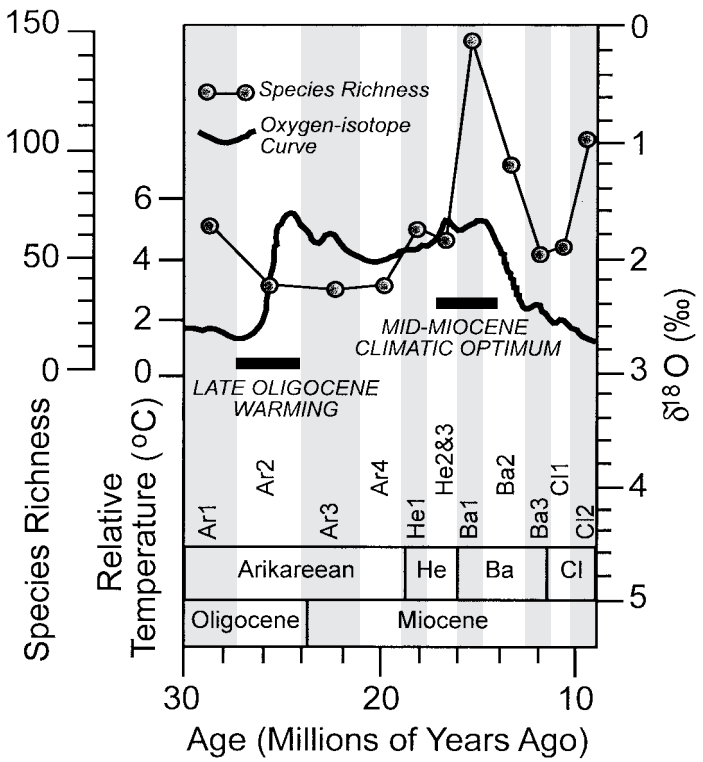

Fig. 1. Time scale (Woodburne and Swisher, 1995) and oxygen–isotope curve (redrawn from Zachos *et al.*, 2001) used in this study. The species richness curve is the composite for all localities, with richness expressed as species per million years. The temperature scale indicates magnitude of change, not temperature reconstructions.

correspond to distinct biogeographic zones that can be defined solely on mammalian species composition: the Columbian (corresponding with NW in Fig. 2), Coloradan (MT) and Kansan (PL) (Hagmeier and Stults, 1964; Hagmeier, 1966). All of the fossil data discussed here occur within one of these three modern biogeographic provinces. The modern mammalian provinces generally correspond with vegetational zones, which, in turn, are linked to climatic parameters and physiographic features (Lugo *et al.*, 1999). Although exact boundaries and similarity indices between biogeographic provinces have undoubtedly changed through time, the Northwest, northern Rocky Mountains and northern Great Plains apparently were distinct biogeographic regions for mammals through much of the Cenozoic (Tedford *et al.*, 1987; Storer, 1989; FAUNMAP Working Group, 1996).

Climate models for assessing pertinent regional differences in Oligo-Miocene climatic parameters do not yet exist. However, general circulation models predict how the modern geographic regions would respond to global climate change, and we examined two of these models to obtain a general sense of whether similarities or differences in specific response among regions might be expected even in the Oligo-Miocene. To assess the range of possibilities, we examined the Hadley Centre and Canadian Climate Centre climate models

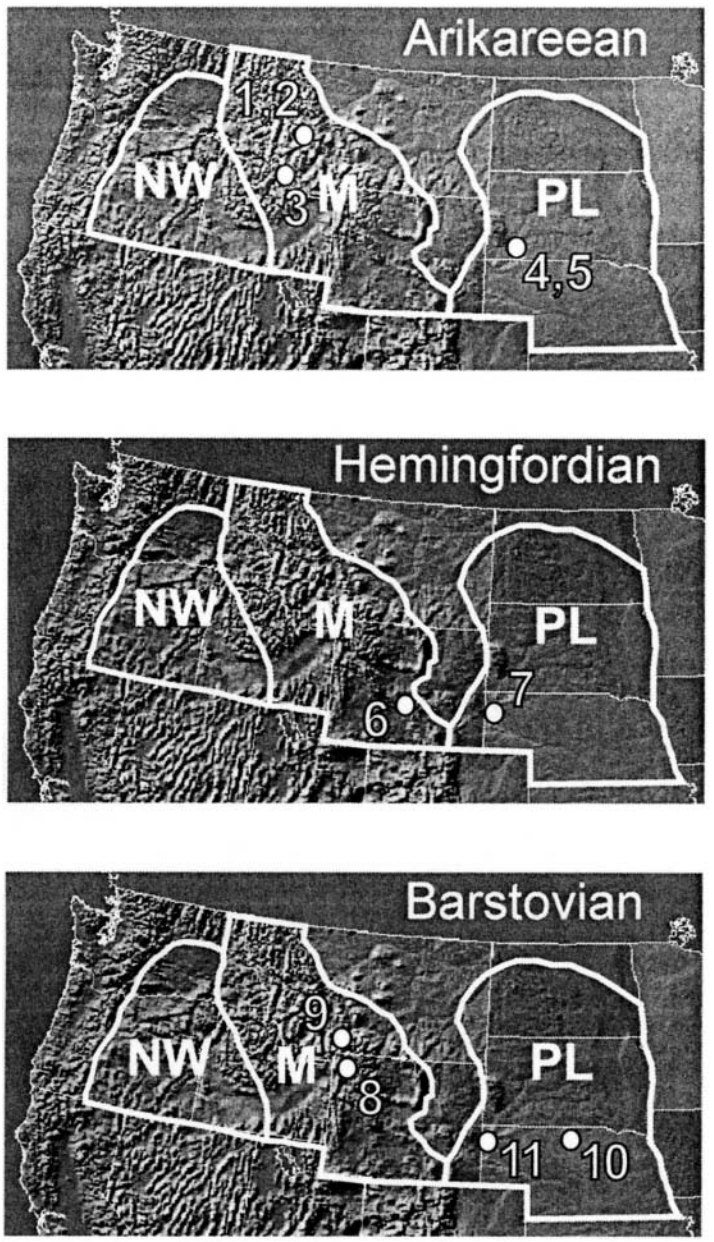

Fig. 2. Boundaries of the biogeographic provinces used for each land mammal age, and location of the specific collecting areas (indicated by numbers) used for the bootstrapping analyses in Figs 6 and 7. *Abbreviations*: NW, Northwest; MT, northern Rocky Mountains; PL, Northern Plains. These roughly correspond to Hagmeier's (1966) Columbian, Coloradan and Kansan mammal biogeographic provinces, respectively. Collecting areas used for bootstrapping analyses are identified by the following numbers: 1, Lower Cabbage Patch Beds: 2, Upper Cabbage Patch Beds; 3, Peterson Creek; 4, Sharps; 5, Monroe Creek; 6, Split Rock; 7, Sheep Creek; 8, Colter; 9, Hepburn's Mesa; 10, E. Norden Reservoir; 11, Olcott. Base maps modified from Sterner (1995).

for effects of a 1% per year increase in greenhouse gases from 2000 to 2100 on average annual temperature, July heat index, summer maximum and winter minimum temperature change, annual precipitation change and summer soil moisture (National Assessment Synthesis Team, 2001). We emphasize that the predictions for climate change in the existing geographic regions are not strictly analogous to what would be expected in the Oligo-Miocene, because ice-sheet configurations, continental elevations, position of Antarctica and, possibly, oceanic circulation patterns are different today. Nevertheless, the models for the modern landscape are useful in determining whether the three regions are geographically close enough (as they were in the Oligo-Miocene) to share some important local responses to a global warming event, or whether markedly different regional responses might be expected.

In general, both models predict that, in response to the stipulated increase in carbon dioxide, the conterminous United States will warm on average between ~2.2°C (4°F) and ~5°C (9°F). All three of the geographic areas of interest are expected to share the following responses: warming of mean annual temperature by 2.7°C (5°F) to 6.7°C (12°F) (temperatures may warm more in the Mountains and northern Plains than the Northwest) and increasing summer maximum temperature by 3°C (5°F) to 6°C (10°F). Potential differences in the way the three regions would respond, seen primarily in the Canadian Model, include: considerably higher (up to 6°C) winter minimum temperatures in the Mountains and Plains than in the Northwest, decreased annual precipitation in the northern Plains (by nearly 20%) versus increased precipitation in the other two regions (by up to 40%), and a greater change in the July heat index in the northern Plains (4°C to 8°C higher). The outlook for summer soil moisture is unclear, as the Canadian and Hadley models present different results.

In general, the two models suggest a mostly similar response to global warming in the three regions (increased annual temperature, increased July maxima and January minima, and increase in the July heat index). Because these three regions were similarly proximal even in the Oligo-Miocene, we assume their generally similar climatic response would have held true then as well. Certainly, however, the exact nature and magnitude of the responses would have been different than today's, given the several differences in boundary conditions. Under this scenario, it would be reasonable to expect parallel changes in species richness as a result of Oligo-Miocene global warming events in the three geographic regions. However, the models for the existing landscape also highlight some possibilities for differential response, notably less winter warming in the Northwest compared to the other two regions, and a considerable increase in the July heat index and decrease in precipitation in the northern Plains. Therefore, the species richness data were also examined to detect discrepancies between the patterns in these three regions.

Estimating species richness began with searching the primary literature (including doctoral dissertations) to identify all reported species occurrences represented by voucher specimens between 30 and 9 million years ago. These include all published information from localities in Washington, Oregon, Idaho, Montana, Wyoming, North Dakota and South Dakota, as well as most published records from Nebraska. Where possible, supplementary specimen information was acquired from online museum databases. For the northern Rockies region, unpublished identified Carnegie Museum specimens from Hepburn's Mesa, Montana, also were utilized. Taxonomy was updated and standardized to conform to McKenna and Bell (1997) for ranks above the genus level and to the latest published

literature for genus and species. The resulting data set includes 721 localities and at least 719 species (Appendix 1).

Species occurrences were entered into a Paradox database that included information about the following attributes: absolute age, relative age, geologic occurrence, taphonomy and literature citations (Barnosky and Carrasco, 2001). The associated absolute and relative age data were used to assign each species occurrence to one of the following biochronologic intervals: Arikareean (Ar) 1, Ar2, Ar3, Ar4; Hemingfordian (He) 1, He2&3; Barstovian (Ba) 1, Ba2, Ba3; Clarendonian (Cl) 1, Cl2 (Woodburne and Swisher, 1995) (Fig. 1). Lack of chronologic resolution required fossils from He2 and He3 to be combined for this study, an appropriate procedure because the temporal interval for the lumped He2&3 is as short or shorter than that of most of the other temporal intervals (Fig. 1). Our Cl1 equates with Woodburne and Swisher's Cl1 plus Cl2, and our Cl2 equals their Cl3; this deviation arose because Woodburne and Swisher did not designate a boundary between their Cl1 and Cl2, so we regarded them as a single biochronological interval. The advantage of the temporal sorting technique was that the age of each locality was evaluated independently using all available geological and biochronological information. Thus there was a high level of confidence that species occurrences were correctly placed within given age intervals. The disadvantage was that it was impossible to sort specimens into very fine, evenly spaced time intervals.

The numerical ages of both the mammal deposits and the oxygen–isotope curve used in this study were ultimately derived by correlation to the standard geomagnetic polarity time scale (Berggren *et al.*, 1995). Zachos *et al.* (2001) reviewed the age models of each of the cores used in their derivation of the oxygen–isotope curve and updated ages as necessary. We also updated as necessary assignments of biostratigraphic age for each of the mammal localities and used the most recent synthetic correlations of the land-mammal ages to the geomagnetic polarity time scale (Woodburne and Swisher, 1995; Berggren *et al.*, 1995). Thus, there is internal consistency of using the best available information for each of the two data sets and tying numerical ages to a common time scale. However, correlations between marine and terrestrial deposits are notably circuitous, and the sampling intervals for the marine cores are clearly much finer than is possible for terrestrial deposits. In fact, the mammal species richness values obtained for each biostratigraphic interval represent a time-averaged sample over a million or more years (i.e. the length of the particular biostratigraphic interval). We assume that this time-averaging of the mammal signal does not substantially affect comparisons to the oxygen–isotope curve for most of the biostratigraphic intervals, because the oxygen–isotope curve does not change dramatically within those intervals. Exceptions are Ar2, within which the Late Oligocene Warming is contained, and Ba2, which contains the transition from the Mid-Miocene Climatic Optimum towards cool global temperatures that characterized the rest of the Cenozoic. Aliasing effects – that is, obscuring the true relationship between two time series by sampling each at different time intervals – could be important in these two biochronological zones. We explore those ramifications further in appropriate parts of the Discussion.

Species richness was first estimated by standardizing the number of species in each interval to species per million years (the quotient of how many species are present in each interval divided by the length of the interval) to correct for biases introduced by differing interval lengths as discussed by Alroy (2000) and Barnosky (2001). Because interval length may not be an accurate proxy for preservation within a time interval, species richness was

also estimated by standardizing the number of species in each interval to species per locality (the quotient of how many species are present in each interval divided by the total number of localities within each interval). Both of these methods yielded estimates for total species richness within and across the large biogeographic regions of focus. A third procedure was used to estimate diversity of discrete, relatively small areas within the larger biogeographic regions. This began with tabulating the numbers of identified specimens (NISP) that were collected at geographically and stratigraphically discrete localities. The NISP was considered an estimate of the number of individuals, and the composite assemblages of fossils from one locality (such as one lens within the Hepburn's Mesa Formation) were considered samples. The samples from each general collecting area (for example, the entire Hepburn's Mesa Formation) were successively pooled to build a species accumulation curve using the bootstrapping algorithms of Colwell (1997). Various problems arise from applying fossil data to the Colwell algorithms and are discussed in more detail in the Discussion. Because many of the Northwest localities lacked published specimen data, only the northern Rockies and the Plains yielded data amenable to bootstrapping estimates of species richness. The collecting areas that yielded the requisite data are noted in Figs 2, 6 and 7. Barnosky (2001) provides additional discussion of methods, as well as details for analyses of the Rocky Mountain collecting areas. All estimates are for the minimum number of species, because specimens that were identifiable to genus but not to species were assumed to belong to specifically identified congeners.

RESULTS

Fluctuations in species richness, calculated as total species divided by duration of the time interval sampled, did not show a strong correlation with climate change through time (Figs 1 and 3). Despite this apparent lack of correlation, all three individual species richness curves (Fig. 3) displayed a concordant signal. The pronounced Late Oligocene Warming in Ar2 was accompanied by almost no change in richness for the Mountains, a slight decrease in the Northwest and a more marked decrease in the Plains. On the other hand, a major increase in species richness in all three regions coincided with the warmest part of the Mid-Miocene Climatic Optimum 17 to 14 million years ago. The fact that species richness did not change in the same direction during the two separate warming events argues against mean global temperature change itself strongly affecting species richness in the three geographic regions. However, the concordant signal in all three regions (Fig. 3) was consistent with expectations for a uniform climatic signal that may be important in the three regions but is not reflected in the global signal. In addition, because of the similar signal in all three regions, combining the data into one curve for the northwest quarter of the USA produced essentially the same pattern, but with higher total numbers of species (Fig. 1).

Caution is warranted in interpreting the patterns in Fig. 1, however, because estimating species richness as species per time interval may be strongly affected by differing numbers of localities in each time interval. Correlation analyses indicated that this is possibly the case for our data. The relationship between total species and length of time interval is non-significant ($r = 0.298$, $P = 0.302$). In contrast, the relationship between total species and number of localities in each time interval is highly significant ($r = 0.771$, $P = 0.001$). Therefore, species per million years does not accurately compensate for biases in preservation, namely, how many localities are known for each time interval. To guard against this potential effect biasing the conclusions, we also constructed richness curves using an

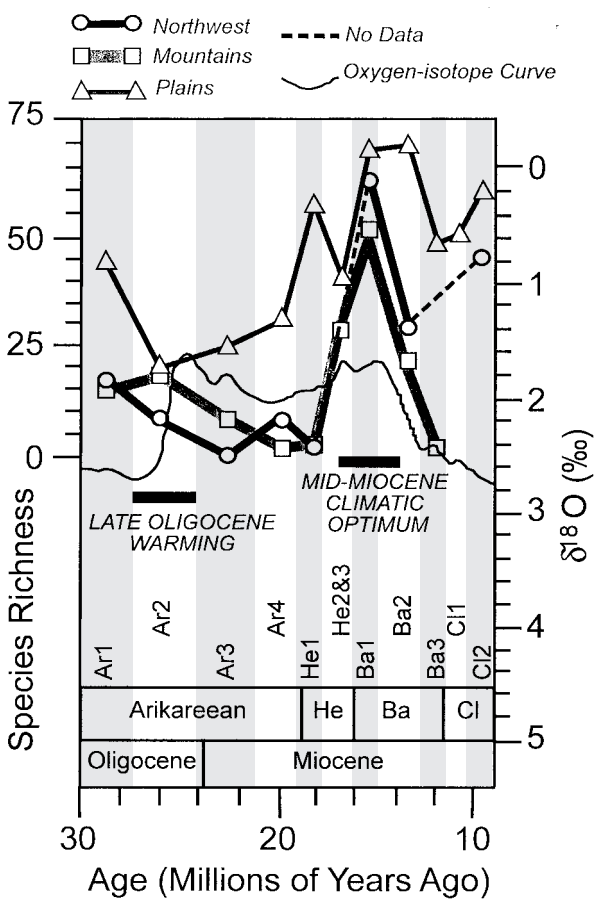

Fig. 3. Region-by-region species richness curves overlaid on the oxygen–isotope curve. See Fig. 1 for further explanation.

alternative proxy for species richness – species per locality (the total species divided by the number of localities in each time interval). This metric is a ratio in which both the numerator and denominator tend to increase as more data are accumulated. This means that small differences in the metric reflect large differences in the numbers of species relative to the numbers of localities.

As was the case for the species per million year curves (Fig. 3), the species per locality curves showed no relationship with climate change through time (Fig. 4). During the Late Oligocene Warming, species per locality increased slightly in the Plains, decreased slightly in the Mountains and underwent a sharp drop in the Northwest. Unlike in Fig. 3, the regional Mid-Miocene Climatic Optimum diversity curves are discordant: little change occurred in the Plains and Northwest in Ba1, whereas a large jump was seen in the Mountains. Neither the Hadley nor the Canadian global climate models predicted a markedly disparate climate signal in the Mountains region relative to the northern Plains and Northwest during a warming event given modern boundary conditions. The discordant species richness pattern

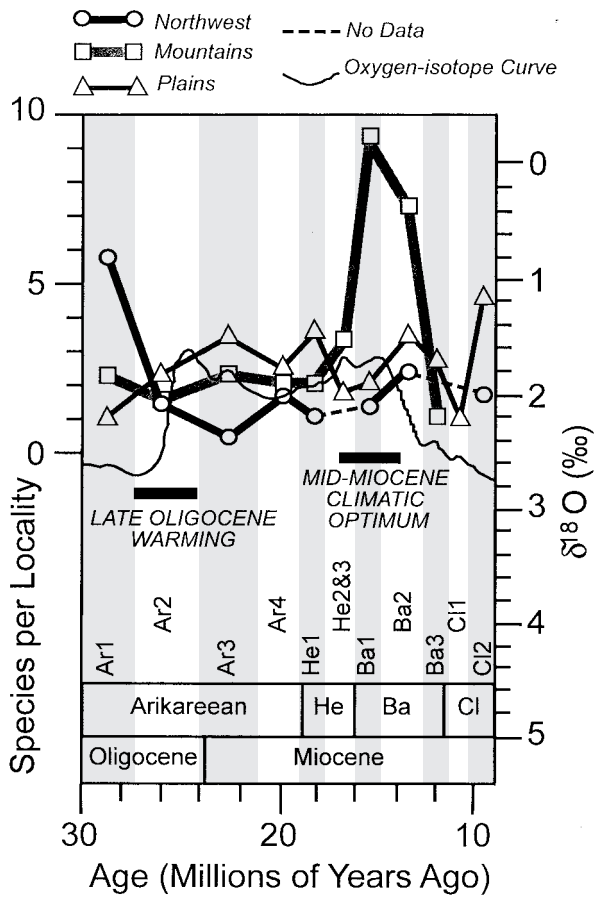

Fig. 4. Region-by-region species diversity curves, with diversity expressed as species per locality, overlaid on the oxygen–isotope curve. See Fig. 1 for further explanation of the oxygen–isotope curve.

evident in Fig. 4 would be unexpected if a similarly uniform climate signal in all three regions was driving species richness in the Oligo-Miocene.

This peak in the Mountains region may be an artifact of having relatively few ($n = 6$) Ba1 localities. It so happens that one of these (Anceney) yielded thousands of specimens and is relatively species-rich. Adding more localities that were less species-rich, perhaps because they were less well-sampled, might be expected to lower the value for species per locality. However, even doubling the number of localities (to 12) and adding no new species would leave a Ba1 peak above the background level for the Mountains curve. The number of localities would have to be tripled (to 18) and no new species added from those localities to remove the peak. This is an unlikely eventuality, especially given the endemism that seems apparent within the Mountains during the Barstovian (see below). For these reasons, while sampling issues may contribute to the peak within the Mountains curve, sampling is unlikely to provide the whole explanation.

Combining the individual regional curves into one curve (Fig. 5) produced an unexpected pattern that did not simply magnify the regional patterns. Instead of high diversity in Ba1,

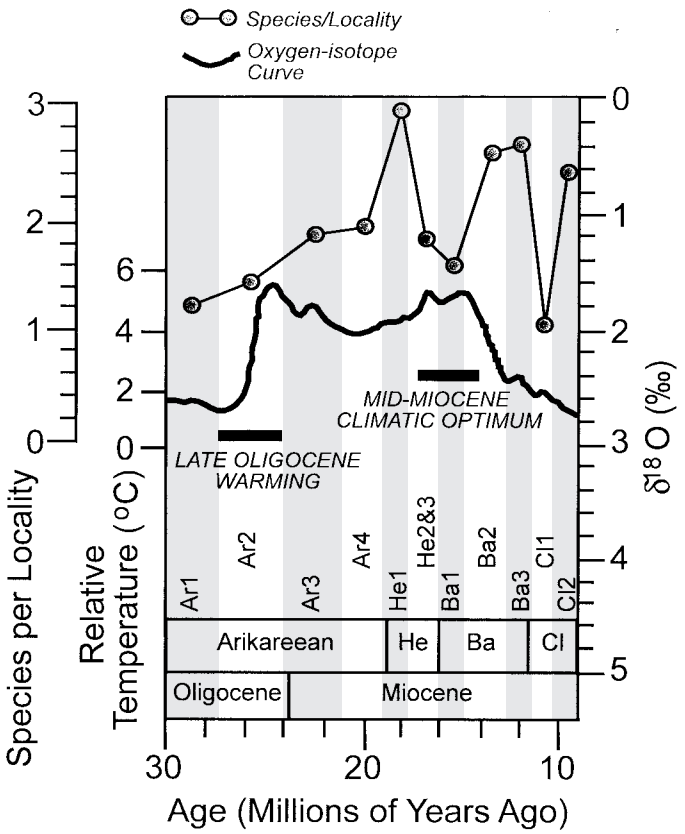

Fig. 5. Composite species diversity curve of all three biogeographic regions overlaid on the oxygen–isotope curve. Species diversity is expressed as species per locality. See Fig. 1 for further explanation of the oxygen–isotope curve.

the combined curve peaked in He1 and fell precipitously in Ba1. The differences between Figs 4 and 5 are the result of between-region differences in species composition. Among regions in He1, species composition varied greatly; that is, each region had a largely distinct set of species. This led to an apparent peak in diversity during He1 in the composite curve (Fig. 5), even though diversity within each region was not particularly high during that interval (Fig. 4). During Ba1, the Mountains had many more species than they did earlier, but many of these species were shared with the Plains and Northwest. This factor – more shared species between regions – acted to depress the composite curve in Ba1 (Fig. 5).

The curves shown in Figs 1, 3, 4 and 5 reflect the compiling of species from many different collecting areas within a given geographic region. High richness could result from high beta diversity but low alpha diversity, high alpha diversity but low beta diversity, or both high alpha and beta diversity. To gain some insight into which aspects of diversity may have changed through the Late Oligocene Warming compared with the Mid-Miocene Climatic Optimum, species accumulation curves were produced by bootstrapping techniques (Colwell, 1997) for collecting areas and localities for which data were available

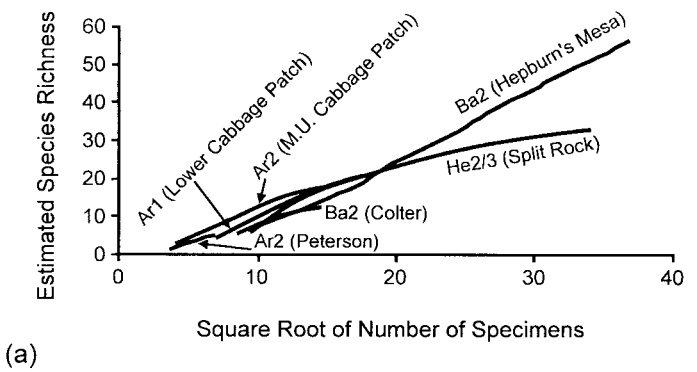

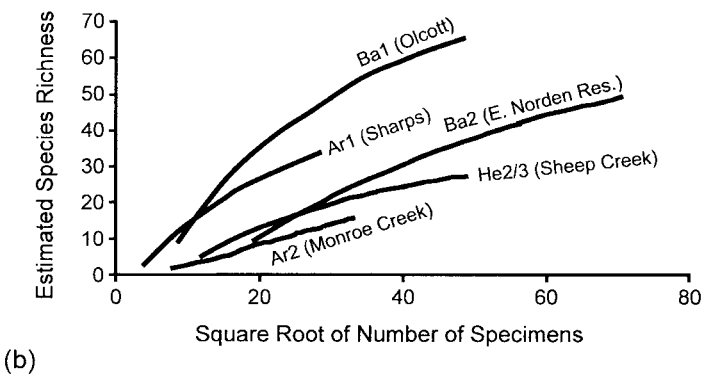

Fig. 6. Bootstrapping estimates of species accumulation curves. Values for species richness are expressed as the quotient of the estimated total species divided by the maximum length of time that could be spanned by the pertinent collecting area. In most cases, this is the entire length of the biochronological age. (a) Bootstrapping curves for the Mountains region; (b) bootstrapping curves for the Plains region. See Fig. 2 for location of samples.

(Figs 6 and 7). These curves provide a perspective on alpha diversity because they depict diversity within one collecting area.

The bootstrapping analysis was first plotted with species richness divided by the maximum length of time that could be spanned by samples in a given collecting area (Fig. 6). In most cases, this corresponded to the length of the relevant biochronological subdivision (e.g. Ar1). This analysis provided no evidence for differences in species richness between Ar1, Ar2, He2&3 or Ba2 for the Mountain localities (Fig. 6a). The Plains localities (Fig. 6b) exhibited a distinct decrease in alpha diversity from Ar1 to Ar2 (across the Late Oligocene Warming), then potentially rose as high as Ar1 values in Ba1 (coincident with the Mid-Miocene Climatic Optimum), then decreased in Ba2. The low diversity for Sheep Creek may represent a taphonomic bias characterized by preservation or collection of predominantly large mammals, although the same collection techniques were used at Olcott. Comparison of Figs 6a and 6b indicates: (1) that the alpha diversity patterns in the two regions differed through time; and (2) that peak alpha diversity did not

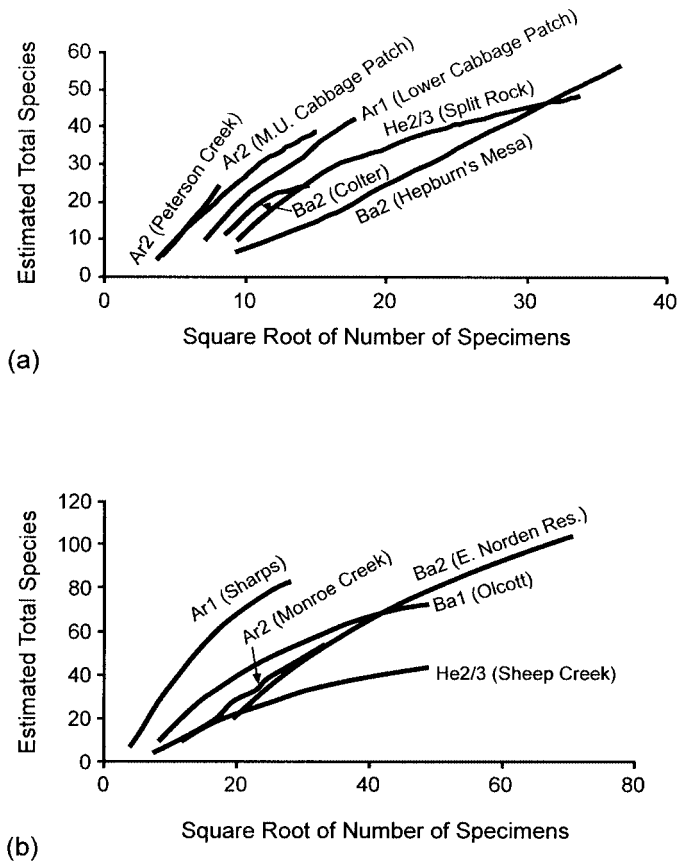

Fig. 7. Bootstrapping estimates of species accumulation curves. The time spanned by each set of samples is assumed to be equal. (a) Bootstrapping curves for the Mountains region; (b) bootstrapping curves for the Plains region. See Fig. 2 for location of samples.

coincide with the Mid-Miocene Climatic Optimum in the Mountains, but may have in the Plains.

The second bootstrapping analysis (Fig. 7) assumed that each collecting area used in the procedure represented an approximately equal amount of time. That is, a given collecting area in the Arikareean was assumed to represent the same amount of time as a given collecting area in the Hemingfordian or Barstovian. Under this assumption, alpha diversity in the Mountains (Fig. 7a) corresponded well with what would be expected if global warming caused changes in species richness during the Late Oligocene Warming: an increase in diversity from Ar1 to Ar2. The Mid-Miocene Climatic Optimum was the time of lowest alpha diversity in the Mountains (He2&3, Ba2). The lowest alpha diversity also appeared during the Mid-Miocene in the Plains data set (Fig. 7b). Like the Mountains data set, the Plains data also showed a change in diversity from Ar1 to Ar2, but in the opposite direction. These data suggest that there was no Mid-Miocene peak in alpha diversity in either region, and that species richness responded oppositely to the Late Oligocene Warming in the Plains and Mountains.

DISCUSSION

Three important questions arise from these results: (1) To what extent might sampling biases be producing a pattern with no biological meaning? (2) If the signal is real, how do the regional patterns compare with continent-wide patterns? (3) What insights do these data provide on how global warming events affect species richness?

A major feature of our first data analysis, using species per million years as our measure of species richness, is the peak in species richness during the Mid-Miocene Climatic Optimum (Figs 1 and 3). However, as discussed, a potential bias in estimating species richness from simply counting up numbers of species per time interval is that richness generally is correlated with numbers of localities (and ultimately numbers of specimens) known from the interval (Alroy, 2000). In the data set reported here, much of the variation in species richness was correlated with numbers of localities included in a given time interval and not related to interval length, the common method of standardization for species diversity analyses. This lack of correlation to the lengths of subdivisions of land mammal ages might be expected because these subdivisions are based on the first appearance of taxa – more localities lead to more taxa and more subdivisions. Therefore, shorter subdivisions are likely to have better preservation, better temporal resolution and greatly exaggerated values for species per million years relative to longer, more poorly sampled subdivisions. This conclusion is supported by the drastically different curves produced using species per million years versus species per locality (Fig. 3 *vs* 4). Species richness measures that employ per million years standardization should therefore be used with caution.

Neither analysis suggested a dramatic change in species richness at the Late Oligocene Warming. We cannot discount aliasing in obscuring the relationship between the mammal data and the temperature signal and, therefore, the conclusion of no change in species richness coincident with climate change during Ar2 is far from firm. If most of the Ar2 mammal localities in fact fall in the early part of the interval, no change in species richness would be expected in our analyses even if species richness fluctuated in lockstep with the global climate curve. In the case of a strong correlation between signals with mammal localities distributed evenly throughout the interval, the change in species richness relative to Ar1 would be dampened, although probably still detectable. Only if most of the localities fell in the latter half of Ar2 would the full magnitude of highly correlated temperature and average mammal signals be apparent relative to Ar1. Independent stratigraphic control presently is not good enough to sort out this problem. Even in view of this, however, it would be difficult to discount the fact that the position of the species richness curve relative to the oxygen–isotope curve is so different in the Late Oligocene Warming compared with the Mid-Miocene Climatic Optimum.

The other interval in which aliasing could be important is during Ba2. The beginning of the interval witnesses some of the warmest temperatures of the entire Oligo-Miocene, but by the end average global temperature was nearly as cool as during Ar1. Interpretations thus range from assuming that most mammal localities fall in the beginning of the interval and that high species richness occurred when temperatures were warm, to assuming that most localities fall near the end of the interval and high richness occurred when temperatures were cold. In either case, the discordance in species-richness patterns between regions (Fig. 4) would be hard to attribute to aliasing alone.

To explore further whether aliasing could somehow be erroneously showing no relationship between the two curves when in fact a correlation existed, we used data

provided by Alroy *et al*. (2000) to determine an average oxygen–isotope value for each of our intervals. We then tested for correlation between the average oxygen–isotope value and the average species-richness value for both species per million years and species per locality. We found no significant correlations, which agrees with the results of Alroy *et al.* (2000) when they performed a similar analysis on data binned into uniform 1 million year intervals.

The lack of a peak at 16–17 million years in the cumulative species per locality curve (which peaks at about 18 million years) and in the regional Plains and Northwest data (trough at 15–17 million years) contradicts the results of some previous continental species curves compiled using different techniques. Stucky's (1990) analysis of continental generic richness through the Cenozoic recognized a peak in generic richness corresponding with the Mid-Miocene Climatic Optimum, around 16 million years ago. Alroy (2000) and Alroy *et al.* (2000) tried to correct for different sampling intensities in constructing continental richness curves and computed richness for lineages rather than for species. They tried to resolve more finely the age assignment of species with a protocol based on conjunction analysis (Alroy, 1992, 1994), which provided estimates of richness at 1 million year time slices. Those studies also noted a peak in continental richness at the Mid-Miocene Climatic Optimum (16–17 million years). Also in contrast to the results presented here, the curves of Alroy (2000) and Alroy *et al.* (2000) suggest highest richness at about 26 million years ago. This corresponds with the times of relatively low richness in Figs 4 and 5.

The different interpretations of Miocene and Oligocene diversity patterns as depicted by Alroy and Stucky and Figs 4 and 5 could reflect biological reality. Under this scenario, diversity would have remained more or less constant in the Northwest, northern Rockies (in the Oligocene only) and northern Plains. The peaks in the Alroy and Stucky curves would therefore have to arise from diversity increases in the Far West, Great Basin, south-central Rockies and south-central Plains, with perhaps some contribution from the northern Rockies. Alternatively, the different techniques of building the curves in this study versus the Alroy and Stucky studies may lead to different results (Stucky, 1990; Alroy, 2000).

Our species per locality regional results do indicate a peak in diversity in the Barstovian (Ba1 and Ba2, ~14 to 15 million years ago) in the Mountains. This is about 1 million years later than the peaks in the Alroy and Stucky continental curves. The Ba1–Ba2 peak in Mountain diversity is consistent, however, with the results of Barnosky (2001), who plotted locality-by-locality species richness against numbers of identifiable specimens per locality for Rocky Mountain localities of relevant ages and found the slopes of the Mid-Miocene Climatic Optimum data to be steeper than the slopes derived from the localities that spanned the Late Oligocene Warming.

Such discrepancies and points of agreement between studies highlight some productive areas for future research that are beyond the scope of the present paper. They also strongly underscore the utility of analysing species-diversity data on a region-by-region basis.

The estimates of alpha diversity (Figs 6 and 7) are subject to several biases. Foremost is that the algorithms used to produce the curves were designed for controlled experimental data. That is, each sample ideally should be of equal size and accumulated the same way, species should be reliably identified from complete individuals, and individuals should be precisely counted. Clearly, none of these assumptions hold true with fossil data. In the analysis reported here, the sample size issue was addressed by examining richness as a function of numbers of identified specimens (NISP), rather than as a function of numbers of samples. The fossils that ultimately contribute to an analysed palaeontological sample

filter through a complex taphonomic pathway that includes mode of death, probability of preservation and collecting technique. As much as possible, localities included in the bootstrapping analyses were those that evidenced reasonably similar taphonomic pathways. Using NISP as a counting technique obviously overestimates the numbers of individuals and, therefore, affects the shape of the curves, but this bias is constant for all samples. Thus while it would not be valid to compare these curves to those produced from sampling individuals from a modern fauna, it is appropriate to compare the palaeontological curves to each other. Bigger problems are introduced from assumptions about the amount of time each sample averages. If the set of samples from one collecting area spans substantially more time than the set of samples from a second collecting area, richness is apt to be greater due to accumulation of species through evolution and immigration. One end of the spectrum assumes that each collecting area encompasses the total length of time spanned by the biochronological interval in which it falls (Fig. 6). The other end of the spectrum assumes that each collecting area spans the same amount of time (Fig. 7). It is not yet possible to assess time spans accurately enough to confidently choose one end of the spectrum over the other. Therefore, inferences here do not go beyond interpreting alpha diversity to fall somewhere in the range of possibilities bracketed by the two extreme cases (Figs 6 and 7). Barnosky (2001) discusses further the potential temporal effects for the Mountain localities.

Given these caveats in interpreting the bootstrapping results, Figs 6 and 7 suggest that alpha diversity did not peak during the Mid-Miocene Climatic Optimum in the Mountains (Figs 6a and 7a). For the Plains, the range of possibilities is inconclusive. Under the assumption of unequal time spans for collecting areas, a Mid-Miocene peak is possible (Fig. 6b); under an assumption of equal time spans, the peak disappears (Fig. 7b). For the Late Oligocene Warming, the Mountain curves range from no support for response to warming (Fig. 6a) to an increase in alpha diversity coincident with warming (Fig. 7a). Both Plains curves (Figs 6b and 7b) suggest a decrease in alpha diversity across the Late Oligocene Warming. To summarize, the most robust conclusions from the bootstrapping analyses are that: (1) alpha diversity did not substantially peak in the Mountains during the Mid-Miocene Climatic Optimum; (2) alpha diversity dropped in the Plains during the Late Oligocene Warming; and (3) the patterns of change in alpha diversity through time were different in the Mountains and the Plains.

The lack of evidence for an increase in alpha diversity in the Mountains at the Mid-Miocene Climatic Optimum is of interest in view of the peak richness at that time indicated by Fig. 4 and by Barnosky (2001). As Stucky (1990) and others have recognized, variations in alpha diversity and beta diversity are commonly decoupled. The relatively low Mid-Miocene values for the bootstrap estimates of species richness (Figs 6a and 7a) combined with high values for overall richness (Fig. 4) would result if alpha diversity was low but beta diversity was high. That is, any single sampling locality would be characterized by low richness, but the assemblages of species would differ dramatically from locality to locality. This conclusion is borne out if one plots the localities known by only one sample (such as Anceney) from the Mountains of Ba1 on Figs 6a and 7a. These single-sample diversity estimates for Ba1 plot close to the curves shown for Ba2 and He2/3, yet when species are summed across Mountain localities, the high peak in Fig. 4 results. If this high beta/low alpha diversity was the case, the Mid-Miocene must have been characterized by increased endemism within the Mountains. In accordance with depression of the composite richness curve during Ba1 (Fig. 5), this endemism also must have been characterized by

some areas in the Mountains sharing species with more easterly regions, and others sharing species with more westerly biogeographic provinces. Such changes in provinciality at times of faunal turnover and regionally differentiated changes also have been reported for Eurasian Miocene faunas, and may well represent the norm for what to expect on the subcontinental geographic scale through long spans of time (Fortelius *et al.*, 1996; Werdelin and Fortelius, 1997; Fortelius and Hokkanen, 2001).

The peak richness in the Mountains around 15 million years has been attributed to the onset of the Mid-Miocene Climatic Optimum in the northern Rockies (Barnosky, 2001), but that conclusion now seems less firm in light of the absence of any response in mountain faunas at the Late Oligocene Warming. The Mid-Miocene richness peak also follows closely the break-up of the northern Rockies and the Basin-and-Range into a diverse landscape characterized by high topographic relief over short distances, and the outpouring of huge amounts of bimodal volcanic flows and ash that significantly changed soil compositions across the western United States. Accompanying these events was extension of the Basin-and-Range that led to increasing its area by some 50% or more (Smith and Braile, 1994). It is tempting to speculate that these tectonic events stimulated faunal diversification directly and indirectly by introducing geographic barriers and changing selection pressures for many taxa. Differences between the regional curves in Fig. 4 and the composite curve in Fig. 5 are consistent with this speculation. During the Hemingfordian and Barstovian, the composite curve does not appear to reflect the changes seen in the regional curves. This lack of reflection would arise if the Mountain fauna shared more species with other biogeographic provinces (e.g. became regionally more pandemic) at some times (low points on Fig. 5) and was regionally less pandemic at others (high points on Fig. 5) relative to the northern Plains and Northwest. At the same time the Mountains exhibited regional pandemism (Ba1, Fig. 5), we see evidence for periods of increased endemism within the Mountains (high beta/low alpha diversity) (Figs 6 and 7). This within-province endemism is not seen in the Plains and the Northwest, where the lack of change is consistent with a tectonic link to changes in species richness and endemism, because those areas were not directly topographically altered by tectonism. Despite these suggestive patterns, the effect of tectonism on species richness remains an open question that merits future work.

Alternatively, it may be that climate change initiated faunal changes at the Mid-Miocene Climatic Optimum but not at the Late Oligocene Warming. The Mid-Miocene Climatic Optimum appears to record the crossing of a climatic threshold that apparently was not crossed at the Late Oligocene event. Unique attributes of the Miocene event relative to the Oligocene one include the following (Flower and Kennett, 1994): (1) deep water cooling, indicating major shifts in ocean currents beginning ~16 million years ago; (2) high-amplitude variations in sea level ~16 to 14 million years ago; (3) faunal turnover in planktonic foraminifera from the tropics to high latitudes; (4) evolutionary turnover in benthic foraminiferal assemblages from ~17 to 14 million years ago; (5) invigoration of surface ocean circulation patterns, including strengthening of gyral circulation and oceanographic fronts; (6) the so-called Monterey Carbon Excursion (Vincent and Berger, 1985; Mutti, 2000), which indicates dramatic and episodic changes in how organic carbon was distributed in carbon reservoirs affecting atmospheric partial CO_2 between 17.5 and 13.5 million years ago; (7) changes in deep water circulation; and (8) potentially increased aridity for mid-continental regions including western North America. If crossing this climatic threshold caused regional climatic changes in the northern Rockies, adjacent Plains and Northwest to diverge relative to how the regions reacted to the Late Oligocene event,

climate change could in fact have precipitated the pattern of biotic change we observe. However, even under this scenario, we would not expect to see regional differences in species-richness patterns given the geographic proximity of the three regions then and now. Nevertheless, the relative merits of this hypothesis versus the tectonic one, or, indeed, if the biotic changes we see in the Mid-Miocene reflect an intersection of both tectonic and global climatic thresholds, deserves further testing.

CONCLUSIONS

The information reported here supports the findings of Alroy *et al.* (2000) that the correlation between global temperature change and species richness through time is not strong. In fact, the data strengthen that conclusion by documenting no uniform richness response to major global warming events even within regions that today share a cohesive climate signal and probably also did in the past. One interpretation is that climatic parameters are not important in influencing species richness through time. Alternatively, specific climatic parameters could be important, in which case mean global temperature inferred from the oxygen–isotope curve would not be the relevant proxy.

The most robust signal in the regional data presented here is the peak of richness in the Mountains region during the Mid-Miocene Climatic Optimum. The richness peak seems to be the result of increased endemism, as evidenced by the bootstrapping analyses of alpha diversity. Although the Mid-Miocene richness peak coincides with a global warming event, the absence of a regional richness peak during the more pronounced Late Oligocene Warming or concomitant increases in the northern Plains and Northwest makes it unlikely that global warming itself caused the increase in species richness. The Mid-Miocene also coincided with the tectonic break-up of the western United States, an increase in continental area due to extension of the Basin-and-Range, a pronounced immigration of mammal species into North America from Eurasia (Woodburne and Swisher, 1995) and the crossing of a climatic threshold signalled by the Monterey Excursion and related oceanographic evidence (Vincent and Berger, 1985; Flower and Kennett, 1994; Mutti, 2000). It is easy to derive a plausible scenario of fragmentation of formerly more extensive geographic ranges, changes in selection pressures, competition from immigrants and qualitatively new climatic regimes (due to a larger and topographically higher Basin-and-Range Province, new ocean circulation patterns and different partial CO_2 relative to the late Oligocene event) affecting the northern Rockies. These events would be consistent with increased speciation rates and the addition of ecological niche-space to the landscape. However, such a model requires explicit formulation and testing with well-conceived research designs before acceptance.

Perhaps our most important conclusions are that assessing species richness in fossil data sets remains onerous, and that how richness is assessed very much affects interpretations about climate's role as a driver. Alroy (2000) has demonstrated the variations that can occur by applying different assumptions and analytical filters to data bearing on continental richness patterns. This paper and Barnosky (2001) demonstrate that different assumptions about temporal duration of samples can lead to very different interpretations about alpha diversity, that different methods of standardization of species richness have large effects on beta diversity estimates, and that geographic scaling issues are important in understanding details of how richness changes through time. Many of the critical assumptions lie at the level of the primary field data – for example, how many specimens were collected, what was

the taphonomic situation and what independent evidence can be brought to bear on the amount of time a given lens of rock spans? Hence future studies that combine knowledge of the primary field sites with appropriate statistical techniques are needed to resolve details of the picture that is beginning to emerge.

ACKNOWLEDGEMENTS

This research was an outgrowth of the MIOMAP Project, supported by NSF Grant EAR-9909353 and represents Contribution No. 1766 from the University of California Museum of Paleontology. The junior author was funded in part by an NSF Minority Postdoctoral Fellowship in the Biological Sciences. We thank the following for helpful comments on the manuscript: Edward Davis, Bob Feranec, Samantha Hopkins, Brian Kraatz, Alan Shabel, Mikael Fortelius and an anonymous reviewer. Brian Kraatz and Sabrina Minter helped with data entry.

REFERENCES

Alroy, J. 1992. Conjunction among taxonomic distributions and the Miocene mammalian biochronology of the Great Plains. *Paleobiology*, **18**: 326–345.

Alroy, J. 1994. Appearance event ordination: a new biochronologic method. *Paleobiology*, **20**: 191–207.

Alroy, J. 2000. Successive approximations of diversity curves: ten more years in the library. *Geology*, **28**: 1023–1026.

Alroy, J., Koch, P.L. and Zachos, J.C. 2000. Global climate change and North American mammalian evolution. In 'Deep Time: Paleobiology's Perspective' (D.H. Erwin and S.L. Wing, eds). *Paleobiology*, **26**(suppl.): 259–288.

Barnosky, A.D. 2001. Distinguishing the effects of the red queen and court jester on Miocene mammal evolution in the northern Rocky Mountains. *J. Vertebrate Paleontol.*, **21**: 172–185.

Barnosky, A.D. and Carrasco, M.A. 2001. MIOMAP data structure. http://www.ucmp.berkeley.edu/miomap/DATA-MIOMAP/mmap_data_structure.htm

Berggren, W.A., Kent, D.V., Swisher, C.C., III and Aubry, M.-P. 1995. A revised Cenozoic geochronology and chronostratigraphy. In *Geochronology, Time Scales and Global Stratigraphic Correlation* (W.A. Berggren, D.V. Kent, M.-P. Aubry and J. Hardenbol, eds), pp. 129–132. Society of Sedimentary Geology Special Publication No. 54. Tulsa, OK: Society of Sedimentary Geology.

Colwell, R.K. 1997. EstimateS: Statistical estimation of species richness and shared species from samples. Version 5. User's Guide and application. http://viceroy.eeb.uconn.edu/estimates

FAUNMAP Working Group. 1996. Spatial response of mammals to late Quaternary environmental fluctuations. *Science*, **272**: 1601–1606.

Flower, B.P. and Kennett, J.P. 1994. The middle Miocene climatic transition: East Antarctic ice sheet development, deep ocean circulation and global carbon cycling. *Palaeogeogr., Palaeoclimatol., Palaeoecol.*, **108**: 537–555.

Fortelius, M. and Hokkanen, A. 2001. The trophic context of hominoid occurrence in the later Miocene of western Eurasia – a primate-free view. In *Phylogeny of the Neogene Hominoid Primates of Eurasia* (L. De Bonis, G. Koufos and A. Andrews, eds), pp. 19–47. Cambridge: Cambridge University Press.

Fortelius, M., Werdelin, L., Andrews, P., Bernor, R.L., Gentry, A., Humphrey, L., Mittmann, H.-W. and Viranta, S. 1996. Provinciality, diversity, turnover and paleoecology in land mammal faunas of the later Miocene of Western Eurasia. In *The Evolution of Western Eurasian Neogene Mammal Faunas* (R.L. Bernor, V. Fahlbusch and H.-V. Mittmann, eds), pp. 414–448. New York: Columbia University Press.

Hagmeier, E.M. 1966. A numerical analysis of the distributional patterns of North American mammals. II. Re-evaluation of the provinces. *Syst. Zool.*, **15**: 279–299.

Hagmeier, E.M. and Stults, C.D. 1964. A numerical analysis of the distributional patterns of North American mammals. *Syst. Zool.*, **13**: 125–155.

Janis, C.M., Damuth, J. and Theodor, J.M. 2000. Miocene ungulates and terrestrial primary productivity: where have all the browsers gone? *Proc. Natl. Acad. Sci.*, **97**: 7899–7904.

Lugo, A.E., Brown, S.L., Dodson, R., Smith, T.S. and Shugart, H.H. 1999. The Holdridge life zones of the conterminous United States in relation to ecosystem mapping. *J. Biogeogr.*, **26**: 1025–1038.

McKenna, M.C. and Bell, S.K. 1997. *Classification of Mammals Above the Species Level*. New York: Columbia University Press.

Miller, K.G. and Fairbanks, R.G. 1985. Oligocene to Miocene carbon isotope cycles and abyssal circulation changes. In *The Carbon Cycle and Atmospheric CO_2: Natural Variations Archean to Present* (E.T. Sundquist and W.S. Broecker, eds), pp. 469–486. Geophysical Monograph No. 32. Washington, DC: American Geophysical Union.

Miller, K.G., Fairbanks, R.G. and Mountain, G.S. 1987. Tertiary oxygen isotope synthesis, sea level history, and continental margin erosion. *Paleoceanography*, **2**: 1–19.

Mutti, M. 2000. Bulk $\delta^{18}O$ and $\delta^{13}C$ records from Site 999, Colombian Basin, and Site 1000, Nicaraguan rise (latest Oligocene to middle Miocene): diagenesis, link to sediment parameters, and paleoceanography. *Proc. Ocean Drilling Program, Scientific Results*, **165**: 275–283.

National Assessment Synthesis Team. 2001. *Climate Change Impacts on the United States: The Potential Consequences of Climate Variability and Change, Overview*. Cambridge: Cambridge University Press and http://www.gcrio.org/NationalAssessment/overpdf/overview.html

Rosenzweig, M.L. 1995. *Species Diversity in Space and Time*. Cambridge: Cambridge University Press.

Smith, R.B. and Braile, L.W. 1994. The Yellowstone hotspot. *J. Volcanol. Geotherm. Res.*, **61**: 121–187.

Sterner, R. 1995. Untitled. http://fermi.jhuapl.edu/states/us/us_color.gif

Storer, J.E. 1989. Rodent faunal provinces, Paleocene-Miocene of North America. In *Papers on Fossil Rodents in Honor of Albert Elmer Wood* (C.C. Black and M.R. Dawson, eds), pp. 17–29. Science Series of Los Angeles County Museum of Natural History No. 33. Los Angeles, CA: Natural History Museum of Los Angeles County.

Stucky, R.K. 1990. Evolution of land mammal diversity in North America during the Cenozoic. *Curr. Mammal.*, **2**: 375–432.

Tedford, R.H., Skinner, M.F., Fields, R.W., Rensberger, J.M., Whistler, D.P., Galusha, T., Taylor, B.E., MacDonald, J.M. and Webb, S.D. 1987. Faunal succession and biochronology of the Arikareean through Hemphillian interval (late Oligocene through earliest Pliocene epochs) in North America. In *Cenozoic Mammals of North America: Geochronology and Biostratigraphy* (M.O. Woodburne, ed.), pp. 153–210. Berkeley, CA: University of California Press.

Vincent, E. and Berger, W.H. 1985. Carbon dioxide and polar cooling in the Miocene: the Monterey Hypothesis. In *The Carbon Cycle and Atmospheric CO_2: Natural Variations Archean to Present* (E.T. Sundquist and W.S. Broecker, eds), pp. 455–468. Geophysical Monograph No. 32. Washington, DC: American Geophysical Union.

Werdelin, L. and Fortelius, M. 1997. Biogeographic characterisation of MN unit reference localities. In *Actes du Congrès BiochroM '97* (J.-P. Aguilar, S. Legendre and J. Michaux, eds), pp. 67–73. Mémoires et travaux de l'Institut de Montpellier No. 21. Montpellier: École pratique des hautes études, Institut de Montpellier.

Woodburne, M.O. and Swisher, C.C., III. 1995. Land mammal high-resolution geochronology, intercontinental overland dispersals, sea level, climate, and vicariance. In *Geochronology, Time Scales and Global Stratigraphic Correlation* (W.A. Berggren, D.V. Kent, M.-P. Aubry and J. Hardenbol, eds), pp. 336–364. Society of Sedimentary Geology Special Publication No. 54. Tulsa, OK: Society of Sedimentary Geology.

Zachos, J., Pagani, M., Sloan, L., Thomas, E. and Billups, K. 2001. Trends, rhythms, and aberrations in global climate 65 Ma to present. *Science*, **292**: 686–693.

APPENDIX 1

The following is the list of localities broken down by time interval, state and biogeographic province. *Abbreviations* – States: ID, Idaho; MT, Montana; NE, Nebraska; OR, Oregon; SD, South Dakota; WA, Washington; WY, Wyoming. Biogeographic provinces: MN, Northern Rocky Mountains; NW, Northwest; PL, Northern Plains. See text for time interval abbreviations.

Locality	State	Bio-geographic province	Locality	State	Bio-geographic province
Arikareean 1					
Lower Cabbage Patch Beds – General	MT	MN	Bull Canyon	NE	PL
Lower Cabbage Patch Beds – Ku-Mt-10	MT	MN	Chadron Roadside Locality	NE	PL
Lower Cabbage Patch Beds – Ku-Mt-15	MT	MN	Durnal Locality	NE	PL
Lower Cabbage Patch Beds – Ku-Mt-17	MT	MN	East of Hubbard Gap	NE	PL
Lower Cabbage Patch Beds – Ku-Mt-20	MT	MN	East of Redington Gap	NE	PL
Lower Cabbage Patch Beds – Ku-Mt-22	MT	MN	Hubbard Gap	NE	PL
Lower Cabbage Patch Beds – Ku-Mt-25	MT	MN	Indian Creek	NE	PL
Lower Cabbage Patch Beds – Ku-Mt-31	MT	MN	McManigal Canyon	NE	PL
Lower Cabbage Patch Beds – Ku-Mt-32	MT	MN	Middlebranch Local Fauna	NE	PL
Lower Cabbage Patch Beds – Ku-Mt-55	MT	MN	NE 1/4, Sec. 9, T32N, R56W	NE	PL
Lower Cabbage Patch Beds – Ku-Mt-7	MT	MN	Redington Gap	NE	PL
Lower Cabbage Patch Beds – MV6501	MT	MN	Round Top	NE	PL
Lower Cabbage Patch Beds – MV6625	MT	MN	Roundhouse Rock	NE	PL
White Sulphur Springs	MT	MN	Ruby's	NE	PL
1 mile W of Roundhouse Rock	NE	PL	S 1/2, Sec. 26, T20N, R53W	NE	PL
1 mile W of UNSM Sf-101	NE	PL	Turtle Point	NE	PL
12 miles S of Bridgeport	NE	PL	UNSM Mo-103	NE	PL
3 miles NE of Wright's Gap	NE	PL	UNSM Sf-104	NE	PL
Bedding Canyon	NE	PL	UNSM Sf-105	NE	PL
Between Roundhouse Rock and Birdcage Gap	NE	PL	UNSM Sx-22	NE	PL
Between Shobar and Logan Canyon	NE	PL	West of Redington Gap	NE	PL
Birdcage Gap	NE	PL	Foree	OR	NW
Black Hank's Canyon	NE	PL	Haystack 32	OR	NW

Long View Ranch	OR	NW	Sharps SDSM V5340	SD	PL
Picture Gorge 12	OR	NW	Sharps SDSM V5341	SD	PL
Picture Gorge 20	OR	NW	Sharps SDSM V5345	SD	PL
Picture Gorge 22	OR	NW	Sharps SDSM V5347	SD	PL
Picture Gorge 29	OR	NW	Sharps SDSM V5348	SD	PL
3.5 miles NW of Wanblee	SD	PL	Sharps SDSM V5349	SD	PL
5 miles NW of Wanblee	SD	PL	Sharps SDSM V5350	SD	PL
8 miles S of Porcupine	SD	PL	Sharps SDSM V5351	SD	PL
AMNH ‘Rosebud’ 25	SD	PL	Sharps SDSM V5352	SD	PL
Cedar Pass	SD	PL	Sharps SDSM V5353	SD	PL
East Side of Potato Creek	SD	PL	Sharps SDSM V5354	SD	PL
East of Cedar Pass	SD	PL	Sharps SDSM V5355	SD	PL
East of Rockyford	SD	PL	Sharps SDSM V5356	SD	PL
F:AM ‘Rosebud’ 1	SD	PL	Sharps SDSM V5357	SD	PL
General Sharps	SD	PL	Sharps SDSM V5358	SD	PL
Harris Ranch	SD	PL	Sharps SDSM V5359	SD	PL
Pass Creek	SD	PL	Sharps SDSM V5360	SD	PL
Pinnacles	SD	PL	Sharps SDSM V5361	SD	PL
Quiver Hill Area	SD	PL	Sharps SDSM V5362	SD	PL
Rosebud (Little White River II)	SD	PL	Sharps SDSM V5363	SD	PL
Rosebud (Little White River III)	SD	PL	Sharps SDSM V5365	SD	PL
Rosebud (Little White River)	SD	PL	Sharps SDSM V541	SD	PL
Rosebud Type Locality	SD	PL	Sharps SDSM V5410	SD	PL
SW of Interior	SD	PL	Sharps SDSM V5413	SD	PL
Sharps LACM 1829	SD	PL	Sharps SDSM V542	SD	PL
Sharps LACM 1872	SD	PL	Sharps SDSM V543	SD	PL
Sharps LACM 1997	SD	PL	Sharps SDSM V544	SD	PL
Sharps LACM 2005	SD	PL	Sharps SDSM V545	SD	PL
Sharps LACM 2007	SD	PL	Sharps SDSM V549	SD	PL
Sharps LACM 6412	SD	PL	Sharps SDSM V572	SD	PL
Sharps LACM 6453	SD	PL	Sharps SDSM V6211	SD	PL
Sharps LACM 6457	SD	PL	Sharps SDSM V6218	SD	PL
Sharps LACM 6670	SD	PL	Sharps SDSM V622	SD	PL
Sharps LACM 6677	SD	PL	Sharps SDSM V6220	SD	PL
Sharps SDSM V5339	SD	PL	Sharps SDSM V6221	SD	PL

Appendix 1 – *cont.*

Locality	State	Bio-geographic province	Locality	State	Bio-geographic province
Sharps SDSM V6223	SD	PL	Sharps SDSM V6263	SD	PL
Sharps SDSM V6224	SD	PL	Sheep Mountain	SD	PL
Sharps SDSM V6225	SD	PL	White Earth Creek	SD	PL
Sharps SDSM V6226	SD	PL	Wolff Camp 2	SD	PL
Sharps SDSM V6227	SD	PL	Darton's Bluff	WY	MN
Sharps SDSM V6228	SD	PL	Little Muddy Creek	WY	PL
Sharps SDSM V6230	SD	PL	Spanish Diggings	WY	PL
Sharps SDSM V624	SD	PL	Willow Creek	WY	PL
Arikareean 2					
Peterson Creek, Big Wash	ID	MN	Middle Cabbage Patch Beds – Ku-Mt-54	MT	MN
Peterson Creek, MV 7303	ID	MN	Middle Cabbage Patch Beds – Ku-Mt-56	MT	MN
Peterson Creek, MV 7304	ID	MN	Middle Cabbage Patch Beds – Ku-Mt-57	MT	MN
Peterson Creek, MV 7305	ID	MN	Middle Cabbage Patch Beds – Ku-Mt-69	MT	MN
Peterson Creek, Rodent Wash	ID	MN	Middle Cabbage Patch Beds – Ku-Mt-70	MT	MN
Peterson Creek, South Bluff	ID	MN	Middle Cabbage Patch Beds – Ku-Mt-71	MT	MN
Canyon Ferry 24LC19	MT	MN	Middle Cabbage Patch Beds – Ku-Mt-9	MT	MN
Canyon Ferry 24LC20	MT	MN	Middle Cabbage Patch Beds – MV6504	MT	MN
Canyon Ferry 24LC21	MT	MN	Middle Cabbage Patch Beds – MV6610	MT	MN
Canyon Ferry (Bonebed)	MT	MN	Upper Cabbage Patch Beds – Ku-Mt-21	MT	MN
Canyon Ferry (Earl Douglass Loc.)	MT	MN	Upper Cabbage Patch Beds – Ku-Mt-4	MT	MN
Canyon Ferry Reservoir 24L C18	MT	MN	Upper Cabbage Patch Beds – Ku-Mt-45	MT	MN
Middle Cabbage Patch Beds – General	MT	MN	Upper Cabbage Patch Beds – Ku-Mt-52	MT	MN
Middle Cabbage Patch Beds – Ku-Mt-11	MT	MN	Upper Cabbage Patch Beds – Ku-Mt-8	MT	MN
Middle Cabbage Patch Beds – Ku-Mt-12	MT	MN	Upper Cabbage Patch Beds – MV6551	MT	MN
Middle Cabbage Patch Beds – Ku-Mt-28	MT	MN	Upper Cabbage Patch Beds – MV6609	MT	MN
Middle Cabbage Patch Beds – Ku-Mt-43	MT	MN	Upper Cabbage Patch Beds – Silver Bow	MT	MN
Middle Cabbage Patch Beds – Ku-Mt-44	MT	MN	Spring Creek 1 (Level 1)	MT	MN
Middle Cabbage Patch Beds – Ku-Mt-46	MT	MN	1.5 miles W of Cochran Wayside Area	NE	PL
Middle Cabbage Patch Beds – Ku-Mt-53	MT	MN	Dawes County Fauna (Dw-121)	NE	PL

Drainage of John Day River	OR	NW	Ironcloud Ranch (SDSM V6215)	SD	PL
Haystack 1	OR	NW	Monroe Creek LACM 1862	SD	PL
Haystack 2	OR	NW	Monroe Creek LACM 1873	SD	PL
Haystack 30	OR	NW	Monroe Creek LACM 1964	SD	PL
Haystack 33	OR	NW	Monroe Creek LACM 1978	SD	PL
Haystack 34	OR	NW	Monroe Creek LACM 2018	SD	PL
Haystack 4	OR	NW	Monroe Creek LACM 65130	SD	PL
Haystack 6	OR	NW	Monroe Creek SDSM V592	SD	PL
Merriam's Locality 864	OR	NW	Monroe Creek SDSM V621	SD	PL
Picture Gorge 17	OR	NW	Monroe Creek SDSM V6210	SD	PL
Picture Gorge 19	OR	NW	Monroe Creek SDSM V6222	SD	PL
Picture Gorge 29	OR	NW	Monroe Creek SDSM V625	SD	PL
Picture Gorge 33	OR	NW	Monroe Creek SDSM V627	SD	PL
Picture Gorge 7	OR	NW	Monroe Creek SDSM V629	SD	PL
Round Up Flat	OR	NW	Sharps SDSM V6224	SD	PL
Rudio Creek 2	OR	NW	Turtle Butte (East End)	SD	PL
Schrock's 1	OR	NW	Turtle Butte (West End)	SD	PL
Somewhere on John Day River	OR	NW	Turtle Butte (West Gap)	SD	PL
Weaver's	OR	NW	Yellow Bear	SD	PL
AMNH 'Rosebud' 10	SD	PL	Wildcat Creek	WA	NW
AMNH 'Rosebud' 11	SD	PL	Emerald Lake SR	WY	MN
AMNH 'Rosebud' 12	SD	PL	Bear Creek Mountain (East)	WY	PL
AMNH 'Rosebud' 13	SD	PL	Dog Skull	WY	PL
AMNH 'Rosebud' 8	SD	PL	Sixty Six Mountain (Upper)	WY	PL
East of Porcupine Creek (SDSM V6229)	SD	PL	Tremain	WY	PL
General Turtle Butte	SD	PL			

Arikareean 3

Peterson Creek MV 7306	ID	MN	Haystack 22	OR	NW
Blacktail Deer Creek	MT	MN	10 miles E of Kyle Post Office	SD	PL
North Boulder Valley	MT	MN	10 miles SW of Eagle Nest Butte	SD	PL
East of McCann Canyon Quarry	NE	PL	5 miles S of Kyle Post Office	SD	PL
Mouth of McCann Canyon Quarry	NE	PL	6 miles W of American Horse Creek	SD	PL
Haystack 19	OR	NW	ACM 'Rosebud' 4	SD	PL
Haystack 21	OR	NW	ACM 'Rosebud' 5	SD	PL

Appendix 1 – *cont.*

Locality	State	Bio-geographic province	Locality	State	Bio-geographic province
AMNH 'Rosebud' 14	SD	PL	Goshen Hole H	WY	PL
AMNH 'Rosebud' 15	SD	PL	Goshen Hole I	WY	PL
AMNH 'Rosebud' 16	SD	PL	Goshen Hole J	WY	PL
AMNH 'Rosebud' 19	SD	PL	Goshen Hole K	WY	PL
AMNH 'Rosebud' 20	SD	PL	Guernsey 1	WY	PL
AMNH 'Rosebud' 21	SD	PL	Guernsey 2	WY	PL
AMNH 'Rosebud' 23	SD	PL	Guernsey 3	WY	PL
AMNH 'Rosebud' 3	SD	PL	Guernsey 4	WY	PL
AMNH 'Rosebud' 7	SD	PL	Guernsey 5	WY	PL
Eagle Nest Butte	SD	PL	Guernsey 6	WY	PL
F:AM 'Rosebud' 2	SD	PL	Guernsey 7	WY	PL
Harrison LACM 2012	SD	PL	Guernsey 8	WY	PL
Porcupine Creek Area	SD	PL	Keeline	WY	PL
77 Hill	WY	PL	North Ridge	WY	PL
Goshen Hole A	WY	PL	North of Jeriah	WY	PL
Goshen Hole B	WY	PL	Raw Hide Creek	WY	PL
Goshen Hole C	WY	PL	SE of Lusk	WY	PL
Goshen Hole D	WY	PL	Silver Springs	WY	PL
Goshen Hole E	WY	PL	UVA Breaks	WY	PL
Goshen Hole F	WY	PL	Van Tassell (Lower)	WY	PL
Goshen Hole G	WY	PL	Van Tassell (Upper)	WY	PL
Arikareean 4					
Grasshopper Creek	MT	MN	Shitike Creek Locality RV-7716	OR	NW
Cart Trail Prospect	NE	PL	Shitike Creek Locality RV-7717	OR	NW
Harper Quarry	NE	PL	Warm Springs Locality RV-7314	OR	NW
Morava Ranch Quarry	NE	PL	Warm Springs Locality RV-7605	OR	NW
Mecca Locality LACM (CIT) 37	OR	NW	Warm Springs Locality RV-7608	OR	NW
Shitike Creek Locality LACM (CIT) 37A	OR	NW	Warm Springs Locality RV-7610	OR	NW
Shitike Creek Locality RV-7715	OR	NW	2 miles below Big Spring	SD	PL

AMNH ‘Rosebud’ 17	SD	PL	Rosebud LACM 1830	SD	PL
AMNH ‘Rosebud’ 18	SD	PL	Rosebud LACM 1864	SD	PL
AMNH ‘Rosebud’ 22	SD	PL	Rosebud LACM 1865	SD	PL
AMNH ‘Rosebud’ 24	SD	PL	Rosebud LACM 1993	SD	PL
AMNH ‘Rosebud’ 26	SD	PL	Rosebud LACM 1998	SD	PL
AMNH ‘Rosebud’ 27	SD	PL	Rosebud LACM 2003	SD	PL
AMNH ‘Rosebud’ 28	SD	PL	Rosebud SDSM V554	SD	PL
AMNH ‘Rosebud’ 29	SD	PL	Lay Ranch Beds	WY	PL
AMNH ‘Rosebud’ 5	SD	PL	Rawhide Buttes	WY	PL
AMNH ‘Rosebud’ 6	SD	PL	Royal Valley	WY	PL
Black Bear Quarry II	SD	PL	Sand Gulch	WY	PL
FMNH ‘Rosebud’ 3	SD	PL	Sixteen Mile District	WY	PL
Hemingfordian 1					
Aletomeryx Quarry	NE	PL	UNSM Cr-131	NE	PL
Cottonwood Creek Quarry	NE	PL	UNSM Cr-133	NE	PL
Cottonwood Creek, Nebraska (Dw-117)	NE	PL	UNSM Cr-134	NE	PL
Cottonwood Creek, Nebraska (Dw-118)	NE	PL	UNSM Cr-135	NE	PL
Dry Creek Prospect B	NE	PL	UNSM Cr-136	NE	PL
Dunlap Camel Quarry	NE	PL	Wood’s Canyon Quarry	NE	PL
Hemingford Quarry 7	NE	PL	Mecca Locality RV-7711	OR	NW
Hemingford Quarry 7B	NE	PL	Warm Springs Locality RV-7606	OR	NW
Marsland Quarry	NE	PL	Black Bear Quarry I	SD	PL
Runningwater Quarry	NE	PL	Flint Hill North	SD	PL
Sand Canyon Region	NE	PL	Flint Hill South	SD	PL
UNSM Cr-126	NE	PL	East Pilgrim 5	WY	MN
UNSM Cr-127	NE	PL	Roy Saunders Locality	WY	MN
UNSM Cr-128	NE	PL	Carpenter Ranch Beds	WY	PL
UNSM Cr-129	NE	PL	Horse Creek Quarry	WY	PL
UNSM Cr-130	NE	PL	Jay Em	WY	PL
Hemingfordian 2/3					
1/4 mile E of Foley Quarry	NE	PL	Ashbrook Pasture	NE	PL
23 miles S of Agate	NE	PL	Ashbrook Quarry	NE	PL
Aphelops Draw	NE	PL	Buck Quarry	NE	PL

Appendix 1 – *cont.*

Locality	State	Bio-geographic province	Locality	State	Bio-geographic province
Companion Quarry	NE	PL	Sand Canyon Dawes Clay 2	NE	PL
Conference Quarry	NE	PL	Sand Canyon Quarry	NE	PL
Dry Creek Prospect A	NE	PL	Sand Canyon Region	NE	PL
Dry Creek Prospect D	NE	PL	Stonehouse Draw	NE	PL
East Hilltop Quarry	NE	PL	Thistle Quarry	NE	PL
East Ravine Quarry	NE	PL	Thomson Quarry	NE	PL
Esther Canyon	NE	PL	Ticholeptus tooheyi type locality	NE	PL
Esther Canyon 2	NE	PL	Vista Quarry	NE	PL
Esther Canyon Tributary	NE	PL	Devil's Gate	WY	MN
Foley Quarry	NE	PL	Devil's Gate UCMP V-77155	WY	MN
General Red Valley Member	NE	PL	Love's 22v	WY	MN
Ginn Quarry	NE	PL	Split Rock UCMP V-69190	WY	MN
Greenside Quarry	NE	PL	Split Rock UCMP V-69191	WY	MN
Hilltop Quarry	NE	PL	Split Rock UCMP V-69192	WY	MN
Long Quarry	NE	PL	Split Rock UCMP V-77144	WY	MN
Marshall Ranch	NE	PL	Split Rock UCMP V-77145	WY	MN
Merychippus Draw	NE	PL	Split Rock UCMP V-77146	WY	MN
Middle of the Road Quarry	NE	PL	Split Rock UCMP V-77147	WY	MN
Pliohippus Draw	NE	PL	Split Rock UCMP V-77148	WY	MN
Ravine Quarry	NE	PL	Split Rock UCMP V-77149	WY	MN
Rhino Quarry	NE	PL	Split Rock UCMP V-77150	WY	MN
Sand Canyon Dawes Clay 1	NE	PL	Split Rock UCMP V-77151	WY	MN
Barstovian 1					
Marsh Creek	ID	MN	23 miles S of Agate	NE	PL
Anceney	MT	MN	AMNH 1908 Quarry	NE	PL
Chalk Cliffs 3A	MT	MN	Ashbrook Pasture	NE	PL
Chalk Cliffs Hepburn Ranch	MT	MN	Boulder Quarry	NE	PL
Flint Creek Beds	MT	MN	Camel Quarry	NE	PL
McKanna Spring	MT	MN	Douglas Quarry	NE	PL

East Jenkins Quarry	NE	PL	Beaver Creek Locality	OR	NW
East Sand Quarry	NE	PL	Birch Creek Locality	OR	NW
East Sinclair Draw	NE	PL	Bowden Hills	OR	NW
East Surface Quarry	NE	PL	Bully Creek	OR	NW
East Wall Quarry	NE	PL	Camp Creek Locality	OR	NW
Echo Quarry	NE	PL	Carson	OR	NW
Far Surface Quarry	NE	PL	Confusion Locality	OR	NW
Floor of Mill Quarry	NE	PL	Corral Buttes	OR	NW
Grass Roots Quarry	NE	PL	Cottonwood Creek	OR	NW
Humbug Quarry	NE	PL	Crooked Creek	OR	NW
Jenkins Quarry	NE	PL	Crooked River	OR	NW
Mesoceras Quarry	NE	PL	Devil's Gate UALP 8878	OR	NW
Mill Quarry	NE	PL	Devil's Gate UALP 8879	OR	NW
New Surface Quarry	NE	PL	Devil's Gate UALP 8950	OR	NW
North Wall Quarry	NE	PL	Devil's Gate UALP 8952	OR	NW
Observation Quarry	NE	PL	Devil's Gate UALP 8955	OR	NW
Pocket 34	NE	PL	Devil's Gate UALP 8963	OR	NW
Princeton's 1914 Locality 1000C	NE	PL	Devil's Gate UALP 9051	OR	NW
Prosynthetoceras Quarry	NE	PL	Devil's Gate UALP 9054	OR	NW
Sand Canyon Region	NE	PL	Devil's Gate UALP 9056	OR	NW
Sand Quarry	NE	PL	Devil's Gate UALP 9057	OR	NW
Sinclair Draw	NE	PL	Gateway Assemblage	OR	NW
Sinclair Quarry	NE	PL	Gateway loc. 368	OR	NW
Snake Quarry	NE	PL	General Mascall	OR	NW
Survey Quarry	NE	PL	Grindstone Creek	OR	NW
Trojan Quarry	NE	PL	Guano Lake	OR	NW
Version Quarry	NE	PL	Guano Ranch	OR	NW
West Sand Quarry	NE	PL	Highway Locality	OR	NW
West Sinclair Draw	NE	PL	MacKay Ranch Locality V-4941	OR	NW
West Surface Quarry	NE	PL	MacKay Ranch Locality V-4942	OR	NW
Basin Locality V-4823	OR	NW	MacKay Ranch Locality V-4943	OR	NW
Basin Locality V-4824	OR	NW	Mascall – North of Dayville	OR	NW
Basin Locality V-4945	OR	NW	Mascall Type Locality	OR	NW
Beatty Buttes	OR	NW	Mascall loc. 113	OR	NW
Beatty Buttes II	OR	NW	Mascall loc. 183	OR	NW

Appendix 1 – *cont.*

Locality	State	Bio-geographic province	Locality	State	Bio-geographic province
Mascall loc. 184	OR	NW	Riverside Locality V-4944	OR	NW
McDonald Locality V-4828	OR	NW	Rock Creek Bridge	OR	NW
McDonald Locality V-4946	OR	NW	Rock Creek Locality	OR	NW
Old Schneider Ranch Locality V-4830	OR	NW	Snyder Creek	OR	NW
Old Schneider Ranch Locality V-4831	OR	NW	South Fork Crooked River	OR	NW
Old Schneider Ranch Locality V-4832	OR	NW	South Fork Locality V-4949	OR	NW
Paulina Creek	OR	NW	South Fork Locality V-4950	OR	NW
Riverside Locality V-4833	OR	NW	Sucker Creek	OR	NW
Riverside Locality V-4834	OR	NW	V4830–4835	OR	NW
Riverside Locality V-4835	OR	NW			
Barstovian 2					
Chalk Cliffs 7	MT	MN	F:AM Rocky Ford Quarry	NE	PL
Chalk Cliffs 9	MT	MN	Forked Hills of Hayden	NE	PL
Chalk Cliffs Owl Gully	MT	MN	Hazard Homestead Quarry	NE	PL
Chalk Cliffs South	MT	MN	High in the Saddle Locality	NE	PL
Chalk Cliffs Spring Area	MT	MN	Hottell Ranch Horse Quarry	NE	PL
Ruby River Basin No. 5	MT	MN	Hottell Ranch Main Quarry	NE	PL
Above Middlebranch	NE	PL	Immense Journey Quarry	NE	PL
Achilles Quarry	NE	PL	Jamber Quarry	NE	PL
Al Holman Turtle Locality	NE	PL	Kuhre Quarry	NE	PL
Annie's Geese Cross	NE	PL	Logan Quarry	NE	PL
Carnivore Quarry	NE	PL	Lost Chance Locality	NE	PL
Carrot Top Quarry	NE	PL	Lost Duckling Quarry	NE	PL
Corner's Gap	NE	PL	Mastodon Quarry	NE	PL
Crookston Bridge Quarry	NE	PL	Messengers' Microsite	NE	PL
Deer Fly Locality	NE	PL	Miller Creek	NE	PL
Devil's Gulch Horse Quarry	NE	PL	Myers Farm	NE	PL
Devil's Gulch Quarry	NE	PL	Niobrara River	NE	PL
Egelhoff Quarry	NE	PL	Norden Bridge Quarry	NE	PL

Norden Damsite Locality	NE	PL	Quartz Basin UO 2457	OR	NW
Penbrook Quarry	NE	PL	Quartz Basin UO 2458	OR	NW
Quarry Without a Name	NE	PL	Quartz Basin UO 2461	OR	NW
Railway Quarry A	NE	PL	Quartz Basin UO 2462	OR	NW
Railway Quarry B	NE	PL	Quartz Basin UO 2463	OR	NW
Rhino Skull Quarry	NE	PL	Quartz Basin UO 2465	OR	NW
Rosetta Stone Locality	NE	PL	Quartz Basin UO 2466	OR	NW
Site Cr-121	NE	PL	Quartz Basin UO 2467	OR	NW
Small Falls Quarry	NE	PL	Red Basin UO 2345	OR	NW
Verdigre Quarry	NE	PL	Red Basin UO 2459	OR	NW
Welke Locality	NE	PL	Red Basin UO 2471	OR	NW
West Valentine Quarry	NE	PL	Red Basin UO 2491	OR	NW
Zippy Lizard Quarry	NE	PL	Red Basin UO 2493	OR	NW
General Quartz Basin	OR	NW	Red Basin UO 2495	OR	NW
General Red Basin	OR	NW	Red Basin UO 2496	OR	NW
Kern Basin	OR	NW	Red Basin UO 2497	OR	NW
Oxbow Basin	OR	NW	Red Basin UO 2498	OR	NW
Quartz Basin UO 2453	OR	NW	Skull Spring	OR	NW
Quartz Basin UO 2455	OR	NW	North Bijou Hill	SD	PL
Quartz Basin UO 2456	OR	NW	South Bijou Hill	SD	PL

Barstovian 3

Burge B Quarry	NE	PL	Penny Creek Wt-11	NE	PL
Burge Quarry	NE	PL	Penny Creek Wt-12	NE	PL
Buzzard Feather Locality	NE	PL	Penny Creek Wt-13	NE	PL
Crazy Locality	NE	PL	Penny Creek Wt-15B	NE	PL
Fatigue Locality	NE	PL	Schlagel Creek Locality	NE	PL
Fence Line Locality	NE	PL	Sherman Ranch Locality	NE	PL
Gordon Creek Quarry	NE	PL	Sunrise Locality	NE	PL
June Quarry	NE	PL	Waldo Simons Quarry	NE	PL
Lighthill Locality	NE	PL	Turtle Butte (West Gap)	SD	PL
Lucht Quarry	NE	PL	Two Ocean Lake	WY	MN
Lull Locality	NE	PL	Trail Creek Quarry	WY	PL
Midway Quarry	NE	PL			

Appendix 1 – *cont.*

Locality	State	Bio-geographic province	Locality	State	Bio-geographic province
Clarendonian 1					
23 miles S of Agate	NE	PL	Big Spring Canyon Site 4	SD	PL
Above Burge B	NE	PL	Canyon of Little White River	SD	PL
Above Middlebranch	NE	PL	Deadman	SD	PL
Big Beaver A	NE	PL	Hollow Horn Bear Quarry	SD	PL
Big Beaver C	NE	PL	Mission Fauna	SD	PL
Chokecherry Quarry	NE	PL	Rosebud Agency Quarry	SD	PL
Crooked Creek Locality	NE	PL	Thin Elk 1	SD	PL
Fat Chance Locality	NE	PL	Thin Elk 10	SD	PL
Head of Coon Creek	NE	PL	Thin Elk 11	SD	PL
Jerry Quarry	NE	PL	Thin Elk 12	SD	PL
Leptarctus B	NE	PL	Thin Elk 13	SD	PL
Little Beaver B	NE	PL	Thin Elk 14	SD	PL
Little Beaver C	NE	PL	Thin Elk 15	SD	PL
McGinley's Stadium	NE	PL	Thin Elk 16	SD	PL
North Rim Locality	NE	PL	Thin Elk 2	SD	PL
Olcott Hill	NE	PL	Thin Elk 3	SD	PL
Poison Ivy Quarry	NE	PL	Thin Elk 4	SD	PL
Precarious Quarry	NE	PL	Thin Elk 5	SD	PL
Slump Blocks	NE	PL	Thin Elk 6	SD	PL
South Big Beaver	NE	PL	Thin Elk 7	SD	PL
Upper County Road Locality	NE	PL	Thin Elk 8	SD	PL
West Coon Creek Locality	NE	PL	Thin Elk 9	SD	PL
Wolf Creek V5326	NE	PL	Trilophodon giganteus site	SD	PL
15 miles NE of Rosebud	SD	PL	Turtle Butte (West End)	SD	PL
3 miles E of Rosebud	SD	PL	Turtle Butte (West Gap)	SD	PL
Big Spring Canyon	SD	PL	Wolf Creek V521	SD	PL
Big Spring Canyon Site 11	SD	PL	Wolf Creek V522	SD	PL
Big Spring Canyon Site 13	SD	PL	Wolf Creek V523	SD	PL
Big Spring Canyon Site 14	SD	PL	Wolf Creek V524	SD	PL

Wolf Creek V525	SD	PL	Wolf Creek V5327	SD	PL
Wolf Creek V526	SD	PL	Wolf Creek V5328	SD	PL
Wolf Creek V527	SD	PL	Wolf Creek V5329	SD	PL
Wolf Creek V528	SD	PL	Wolf Creek V5330	SD	PL
Wolf Creek V529	SD	PL	Wolf Creek V5331	SD	PL
Wolf Creek V5321	SD	PL	Wolf Creek V5332	SD	PL
Wolf Creek V5322	SD	PL	Wolf Creek V5333	SD	PL
Wolf Creek V5323	SD	PL	Wolf Creek V5334	SD	PL
Wolf Creek V5324	SD	PL	Wolf Creek V5335	SD	PL
Wolf Creek V5325	SD	PL	Wolf Creek V5336	SD	PL
Clarendonian 2					
Stagestop UALP 8881	ID	NW	Black Butte UO 2336	OR	NW
Stagestop UALP 8964	ID	NW	Black Butte UO 2337	OR	NW
23 miles S of Agate	NE	PL	Black Butte UO 2338	OR	NW
Big Toad Beach	NE	PL	Black Butte UO 2339	OR	NW
Bluejay Quarry	NE	PL	Black Butte UO 2340	OR	NW
Grasz Cat	NE	PL	Black Butte UO 2341	OR	NW
Hesperopithecus site	NE	PL	Black Butte UO 2343	OR	NW
Kepler Quarry	NE	PL	Black Butte UO 2344	OR	NW
Kilpatrick Quarry	NE	PL	Black Butte UO 2348	OR	NW
Lonergan Creek	NE	PL	Black Butte UO 2352	OR	NW
North Shore	NE	PL	Black Butte UO 2353	OR	NW
Olcott Hill	NE	PL	Black Butte UO 2354	OR	NW
Olcott Quarry	NE	PL	Black Butte UO 2448	OR	NW
Pratt Quarry	NE	PL	Black Butte UO 2500	OR	NW
Serendipity Quarry	NE	PL	General Black Butte	OR	NW
Sinclair Draw	NE	PL	Ironside	OR	NW
Black Butte UO 2326	OR	NW	Ironside 2	OR	NW
Black Butte UO 2328	OR	NW	West of Riverside	OR	NW
Black Butte UO 2332	OR	NW	Granger Clay Pit	WA	NW
Black Butte UO 2333	OR	NW	Roza Canal	WA	NW
Black Butte UO 2334	OR	NW	Southern Yakima Canyon	WA	NW
Black Butte UO 2335	OR	NW			